


# Machine learning-based time series analysis of polylactic acid bead foam extrusion

Karim Ali Shah<sup>1</sup> | Rodrigo Q. Albuquerque<sup>1,2</sup> | Christian Brütting<sup>1</sup> |  
Holger Ruckdäschel<sup>1,2</sup> 

<sup>1</sup>Department Polymer Engineering,  
University of Bayreuth, Bayreuth,  
Germany

<sup>2</sup>Neue Materialien Bayreuth GmbH,  
Bayreuth, Germany

## Correspondence

Holger Ruckdäschel, Department Polymer  
Engineering, University of Bayreuth,  
Universitätsstrasse 30, Bayreuth 95447,  
Germany.

Email: [holger.ruckdaeschel@uni-bayreuth.de](mailto:holger.ruckdaeschel@uni-bayreuth.de)

## Funding information

Deutsche Forschungsgemeinschaft,  
Grant/Award Number: RU 2586/5-1

## Abstract

Understanding the behavior of polymer melts during extrusion is essential for optimizing processes and developing new materials. However, analyzing the continuous data generated by an extruder poses significant challenges. This paper investigates the utility of machine learning in predicting melt pressure at the die plate in polylactic acid (PLA) bead foam extrusion, a critical parameter in the extrusion process. Utilizing a random forest (RF) model, we examine how various processing parameters influence melt pressure. By segmenting the data into time-delayed intervals, we achieve accurate predictions. We present forecasts of melt pressure at the die for intervals of 5 s, 1 min, and 5 min, demonstrating particularly strong performance for the 5-min forecast with a Mean Absolute Error (MAE) of 1.88 and the coefficient of determination ( $R^2$  score) of 0.90. By exploring time series data, our study demonstrates the effectiveness of the RF model and provides a foundation for more advanced and precise control strategies in polymer bead extrusion processes.

## KEYWORDS

bead foam extrusion, bead foams, bio-based polymers, machine learning, PLA, polymer foams, time series, twin screw extruder

## 1 | INTRODUCTION

Polymer foams feature unique cellular structures and possess various attributes, including low density, high strength, thermal insulation, damping properties, and sound absorption capacities.<sup>1</sup> Polymer foams have long been essential products, simplifying our daily lives through a wide range of applications. They play crucial roles in numerous industries, particularly in insulation and packaging, owing to their exceptional performance characteristics.<sup>2–4</sup>

Polymer bead foams, a significant category of polymeric foams, have gained considerable attention across various industrial sectors due to their versatile properties and applications. They stand out for their unique features and widespread utility.<sup>5–8</sup> Particularly, polymer bead foams made from polylactic acid (PLA) have garnered significant interest in various industries due to their lightweight nature, biodegradability, and versatility. The biodegradability of PLA bead foams distinguishes them as environmentally friendly alternatives to conventional petroleum-based foams, aligning with the growing

This is an open access article under the terms of the [Creative Commons Attribution](https://creativecommons.org/licenses/by/4.0/) License, which permits use, distribution and reproduction in any medium, provided the original work is properly cited.

© 2024 The Author(s). *Journal of Applied Polymer Science* published by Wiley Periodicals LLC.

emphasis on sustainable practices across industries.<sup>6,9–11</sup> Among the multiple manufacturing processes, extrusion stands out as an essential method for efficiently producing PLA bead foams. However, extrusion processes are characterized by their continuous nature, posing unique challenges in understanding and optimizing the process parameters.

The use of artificial intelligence (AI) will be key to improving the development speed of new products and technologies. Machine learning (ML) has become increasingly vital in the field of AI, playing an important role in revolutionizing various industries and scientific domains.<sup>12</sup> Its significance lies in its ability to analyze vast amounts of data from diverse sources, including machines, devices, sensors, and digital platforms. With the help of advanced algorithms and statistical techniques, ML extracts valuable patterns, trends, and relationships from these datasets, enabling researchers, analysts, and practitioners to derive actionable insights and make informed decisions. To effectively use ML for processes or product development, one needs a substantial amount of data, which depends on the variability and complexity of the process. Despite the abundance of machine learning techniques, the use of digital methods remains quite limited in scientific research for polymer processing.<sup>13</sup>

One of the primary goals of ML is predictive modeling, wherein historical data is utilized to forecast future outcomes or behaviors. Through techniques such as regression analysis, ML algorithms can discern underlying patterns and dependencies within the data, thereby enabling accurate predictions about future events, trends, or system behaviors. These predictive capabilities find applications across numerous domains, including finance, healthcare, marketing, manufacturing, transportation, material production, and more. The growing availability of big data, coupled with advancements in computational power and algorithmic techniques, has propelled the widespread adoption of ML across various sectors. Its ability to uncover hidden insights, optimize processes, and drive innovation has positioned ML as a cornerstone of modern scientific inquiry and technological advancement.<sup>14</sup>

A few attempts have been made to integrate ML techniques into various aspects of polymer science, ranging from polymer synthesis, utilizing high throughput devices,<sup>15</sup> to flow chemistry,<sup>16</sup> and extending to polymer processing and part production.<sup>13</sup> The diverse range of ML approaches underscores their high potential.<sup>17–20</sup> Numerous studies have explored the combination of ML with 3D printing and injection molding techniques.<sup>21,22</sup>

The analysis of continuous processes offers opportunities to expand beyond traditional methodologies,

enabling the application of various models to extensive datasets. Bead foam extrusion, along with other extrusion technologies, is particularly suitable for such analysis due to its continuous nature and well-established technology, which includes numerous temperature and pressure sensors.<sup>6</sup>

In a study by Pech et al.,<sup>23</sup> a neural network-based ML model is utilized to investigate bead foam size parameters of expanded polystyrene foams on compression properties. The model's predictions closely match experimental findings, with a standard deviation of less than 3% relative to the experimental data. Another ML model studied by Piumi et al.<sup>24</sup> predicts the impact of microplastics on soil properties using gradient boost regression (GBR), achieving  $R^2$  values ranging from 0.86 to 0.99.

In recent years, time series analysis-based ML techniques and their applications have gained significant attention across diverse industries and research domains.<sup>25–30</sup> The potential of these techniques is particularly pronounced in the field of material processing.

The emergence of ML techniques has transformed the analysis of time series data, enabling the extraction of valuable insights and predictive capabilities across various domains.<sup>31,32</sup> Within polymer processing, ML-based time series analysis offers promising avenues for understanding the complex relationships between process parameters and product quality. In their study, Andrews et al.<sup>33</sup> employ supervised machine learning techniques to analyze nanoseconds-long time series data, focusing on energy fluctuations in molecular dynamics of polymers. Recent studies have investigated the extrusion processes of PLA bead foam using different ML techniques.<sup>34</sup> Despite extensive research, there is a notable absence of literature addressing the application of time series-based machine learning approaches to polymer bead foams, particularly those composed of PLA.

This paper explores the utilization of ML-based time series analysis specifically tailored for PLA bead foam extrusion. The objective is to predict the future melt pressure at the die plate in the twin-screw extruder in bead foam extrusion process. Melt pressure, a critical parameter in bead foam extrusion, profoundly influences key product attributes such as cell structure, density, and mechanical properties. However, accurately predicting melt pressure poses a formidable challenge due to the complex interdependencies among process variables, material properties, and environmental factors inherent in extrusion processes. We address the challenges presented by PLA bead foam extrusion, including the need for segmentation to accurately identify operational and downtime periods. This will not only aid in isolating meaningful segments for analysis but also facilitate the development of targeted ML models for the bead foam

extrusion process. Additionally, we shed light on the complex process of data collection for time series analysis in continuous manufacturing environments, underscoring the significance of data acquisition strategies.

## 2 | MATERIALS AND METHODS

### 2.1 | Materials

In this investigation, PLA, specifically Ingeo 2003D (NatureWorks Ltd., Minnetonka, MN), was employed. This material is characterized by its high molecular weight suitable for extrusion processes, featuring a D-content of approximately 4.3% and a melting point of 150°C.<sup>35</sup>

### 2.2 | Method

Bead foam extrusion is a continuous process, utilizing a tandem-extrusion line with two interconnected extruders, as shown in Figure 1. The tandem extrusion setup is often favored in industrial-scale operations due to its enhanced dispersion capabilities for blowing agents, chain extenders, and nanoadditives, coupled with temperature control and cooling capacity. In the process of producing PLA bead foams, the material is melted in the twin-screw extruder (A-extruder, L/D = 42 with a screw diameter of 25 mm), after which CO<sub>2</sub> is introduced into the molten material as a blowing agent. The temperature profile as set to 25°C at the hopper to prevent ensure sufficient dosing followed by 160°C for the next heating zones and 180°C for rest of the A-Extruder. The melt and CO<sub>2</sub> are homogenized by the twin-screw extruder to create a homogeneous single-phase mixture. Subsequently,

the melted material is transferred to the single-screw extruder (B-extruder, L/D = 30 with a screw diameter of 45 mm), where it undergoes cooling and temperature equilibration. This cooling process results in an increase in pressure within the B-extruder. Here the temperature was varied between 175 and 140°C. Upon passing through the die and entering the UWG (underwater granulator), the material experiences a significant pressure drop, leading to foaming or expansion. Within the UWG, a rotating knife is utilized to cut the foaming material into beads while maintaining specific water pressure. The schematic diagram of the bead foam extrusion process is presented in Figure 1. The position of the temperature and pressure sensor are also shown here, which are placed right to the Die Plate. The varied processing parameters can be seen in Table 1. The continuous data was selected by extracting the machine protocols and analyzed by python.

### 2.3 | Data analysis

For this study, we utilized a dataset comprising 20,998 data points collected over a four-day trial of the PLA bead foam extrusion process. The bead foam extrusion data was automatically logged into the Siemens Insight Hub<sup>1</sup> software, a comprehensive data management system

TABLE 1 Overview of varied process parameters.

Parameter	Units	Min	Max
Blowing agent	%	0	6
Rotating cutting speed	RPM	2000	4500
Die plate hole (Diameter)	mm	2 × 1.4	1 × 2.8
Die plate temperature	°C	160	190

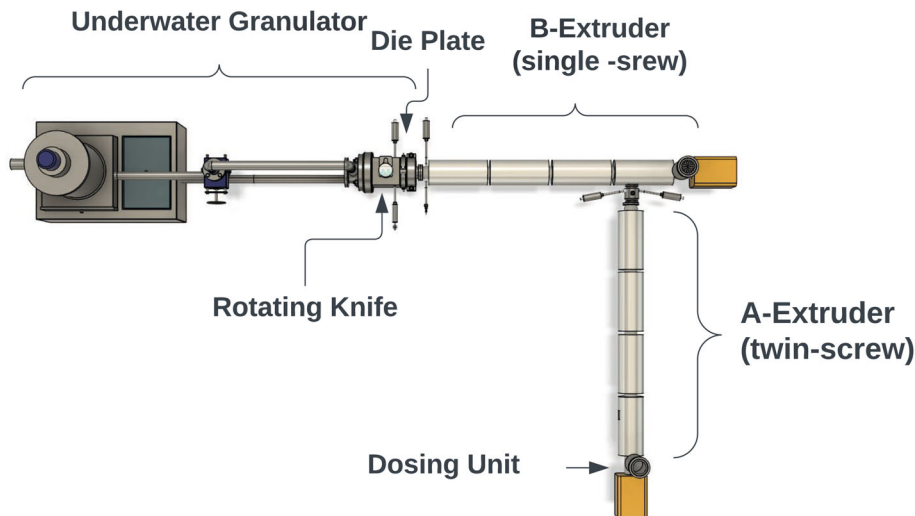


FIGURE 1 Schematic illustration of a bead foam extrusion machine with an underwater pelletizing unit, showcasing key processing components emphasized for clarity. [Color figure can be viewed at [wileyonlinelibrary.com](http://wileyonlinelibrary.com)]

**ALGORITHM 1 Segmentation of time series**

For a given time series  $u_t$ , where  $t = (1, 2, 3, \dots, n)$ , and  $L \in \{50, 100, 200, 300\}$  the segments,

Then, we define a target  $n$  such that for all  $n \in \mathbb{N}$ , and 1 shows a time step in future

$$n = L \cdot u_t + 1 \quad (1)$$

utilizing Excel files to archive daily records. Prior to analysis, the data underwent preprocessing stages to ensure accuracy and suitability for subsequent analysis procedures. The preprocessing encompassed data cleaning to rectify missing values, followed by data transformation aimed at standardizing formats and aligning with the necessary analytical tools, which involve feature engineering to extract relevant information. After the data was preprocessed using different Python's libraries, various analytical techniques were applied to gain insights from the data.

After the data cleaning process, segmentation of the time series data was done. Segmentation is a basic technique used in time series analysis to divide a continuous sequence of data into smaller overlapping subsets or windows. Each segment contains a fixed number of consecutive observations, and a target is associated with each segment, usually positioned immediately after the last observation in the segment. The segment moves along the time series with a specific step size or shift, enabling the creation of multiple overlapping segments. The segmentation process is crucial for organizing the time series data into relevant intervals that capture important processing parameters (Algorithm 1).<sup>36,37</sup>

The segmentation process included the following steps:

1. **Time Windows:** This step involves determining the duration of time windows that best capture the dynamics of the manufacturing process. Criteria were established to segment the time series data into distinct segments length, like 50, 100, 200, and 300.
2. **Shift:** This step defines a shift for the relevant time series determining an offset or displacement parameter that adjusts the temporal alignment of the data, like 30, 50, 70, and 90 shift in this case.

Time series segmentation can also be observed visually in Figure 2, where the time series  $u_t$  is segmented

with a segment length of  $L = 100$ , with shift of 50 to create a dataset. Additionally, the targets are shown for different future time intervals, such as 5 s, 1 min, and 5 min.

**2.4 | Data curation**

The segmented time series data was created, with each segment describing a distinct phase of the manufacturing process characterized by unique processing parameters and operational conditions. Subsequently, a new dataset was constructed, compiling the complete data history for each set of processing parameters. The new dataset underwent curation to ensure its suitability for meaningful observation in machine learning models and forecasting. Data curation is especially crucial in the context of applying machine learning techniques to data analysis, particularly in processing settings such as extrusion processes.

For data curation, we established a threshold value of 75 bar for the melt pressure at the die. This threshold helps identify downtime periods and instances when the pressure falls below 75 bar. Such downtimes not only signal periods of discontinued production but also potentially indicate instances where the extruder has been intentionally shut down for maintenance or other operational reasons. This specific threshold was selected due to its correlation with the stopping of material flow through the extruder, a phenomenon observed when the pressure at the die drops below this level. This relationship is visually represented in Figure 3, where distinct colors distinguish pressure values above (blue) and below (red) the 75 bar threshold. The melt pressure at the die is monitored using an MD1 sensor, strategically positioned at the apex of the die plate, concluding the A-extruder. This sensor boasts a precision tolerance of approximately 1%. Accurate measurement of melt pressure is crucial for maintaining optimal processing conditions and ensuring the consistency of the extruded polymer bead foam.

Given the continuous nature of our time series data and its extensive historical record of processing parameters, we encounter a common challenge associated with data processing, the presence of numerous interrelated parameters. Changes in one parameter can significantly affect others, and this holds true for melt pressure at the die as well. When the pressure exceeds a certain limit, it can trigger machine shutdowns. Therefore, the data curation process becomes essential to retain all valid points for further analysis, ensuring that only valid data are fed into the model.

The models were developed using Python libraries, including NumPy and scikit-learn, within Visual Studio

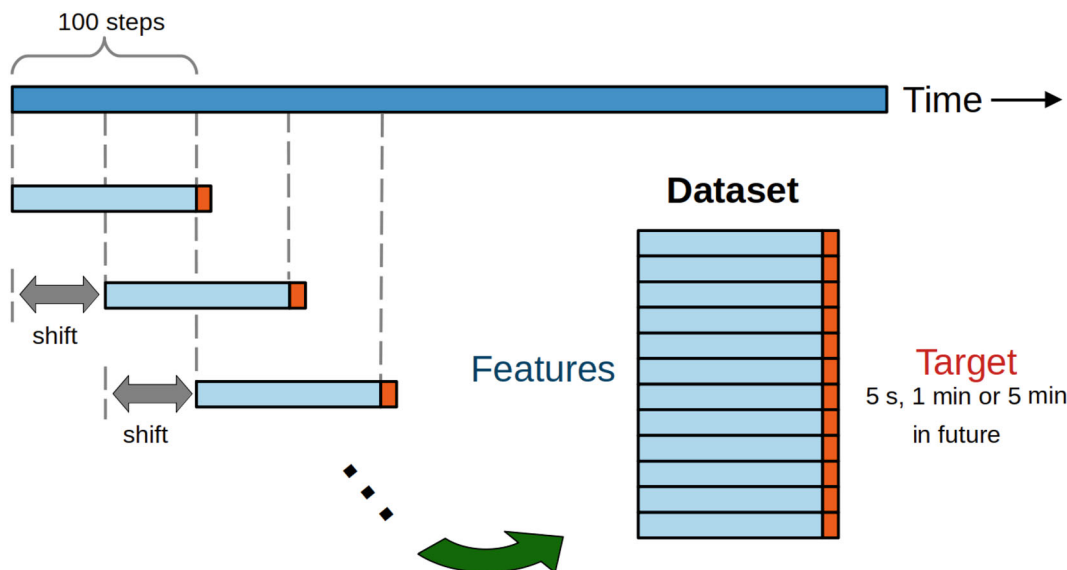


**FIGURE 2** Schematic illustration of the time series segmentation process to create a dataset using a segment length of 100 for the time window and a shift parameter for the target. [Color figure can be viewed at [wileyonlinelibrary.com](https://onlinelibrary.wiley.com)]

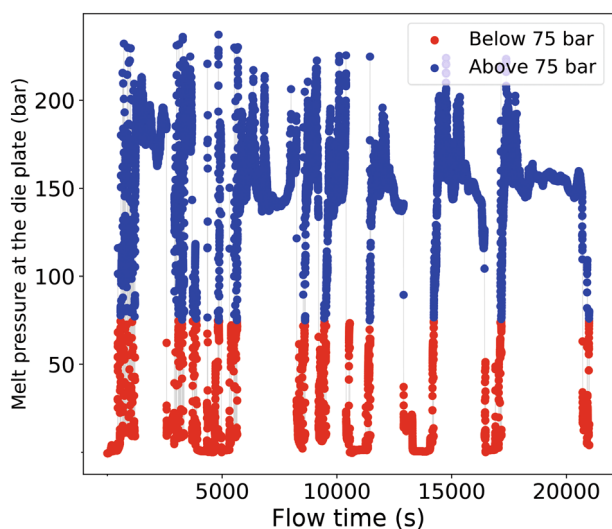


**FIGURE 3** The plot illustrates the variation of the melt pressure at the die over time. The red color indicates values of melt pressure at the die less than 75 bar, representing downtime, while the blue indicates values above 75 bar. [Color figure can be viewed at [wileyonlinelibrary.com](https://onlinelibrary.wiley.com)]

Code, also commonly referred to as VS Code. The code was specifically written in Python 3.12 using VS Code.

## 2.5 | Model training

Multiple machine learning regression models were screened to forecast the target property based on the features. Initially, Decision Tree (DT), Random Forest (RF), Least Squares Regression (LR), and Support

Vector Regressor (SVR) were evaluated. Out of all the ML models, the Random Forest model showed the best results and was selected for further analysis. To evaluate the model performance, 5-fold cross-validation was employed. This approach partitions the dataset into five subsets of equal size. Then, the model is iteratively trained on four subsets and validated on the remaining subset. This process is repeated five times, with each subset used once as the validation set. The average performance across all iterations provides a robust assessment of the model's generalization capability.

We split the data into training and testing sets for the ML model. In the unshuffled scenario, we perform the split without shuffling the data points. Specifically, we allocate 80% of the data for training and the remaining 20% for testing. However, unlike shuffled datasets where the data points are randomly arranged before splitting, in unshuffled datasets, we simply take the first 80% of the data for training the model. Subsequently, we evaluate the trained model's performance using the last 20% of the data as the test set. This approach ensures that the model is tested on data points that occur temporally after the training data, mimicking real-world forecasting scenarios more accurately.

We compiled statistical data for each dataset generated with varying shift and segment parameters. This statistical summary comprises key metrics such as mean, standard deviation, minimum, maximum, as well as the 25th, 50th (median), and 75th percentiles of the dataset. This comprehensive statistical analysis provides valuable insights into the distribution and variability of the data

across different experimental configurations, facilitating a deeper understanding of the forecasting results.

## 2.6 | Metrics

We employed two key metrics, the coefficient of determination ( $R^2$ ) and the mean absolute error (MAE), to evaluate the performance of the model.

These metrics offer insights into the precision and accuracy of the predictions made by each model:

1.  $R^2$  score represents the proportion of variance in the target variable (melt pressure at the die in bar) that can be explained by the models. A score closer to 1.0 signifies a stronger fit between the predicted and actual values.
2. MAE measures the average magnitude of errors between the predicted and actual values. Lower MAE values indicate higher accuracy in forecasting.

## 2.7 | Optimizing time settings

Our initial analysis began by segmenting the data with a length of 300 and a shift of 50 to forecast the melt pressure 5 s into the future. This choice was guided by the frequency of data collection, which occurred at 5-s intervals. Thus, initiating the forecast at 5 s allowed for a natural progression in our analysis. For this specific combination of shift and segment length, the MAE was found to be 3.49. This average MAE includes four individual MAE values corresponding to shuffled, unshuffled, statistically shuffled, and statistically unshuffled data. Furthermore, we conducted analyses with decreasing segment lengths, including 200, 100, and 50. Figure 4 depicts a contour plot illustrating the optimization of time settings, with the dark blue region indicating the best parameter combination. Additionally, the shift parameter was considered alongside segment length. The overview of the all the data and corresponding MAE can be seen in Table 2. For further insights into the forecasting performance, detailed MAE and  $R^2$  values for each segment are provided in the Supporting information (Data S1).

The experiments were continuously monitored, where signals were recorded every 5 s during many hours and for different days. The choice of 5 s, 1 min, and 5 min for which predictions were performed in advance, lies in the fact that they provide a reasonable range involving the shortest time step (5 s) and a much longer one (5 min). Although other time ranges could have been used, the current one allowed for a proof-of-concept investigation, which was the aim of this study.

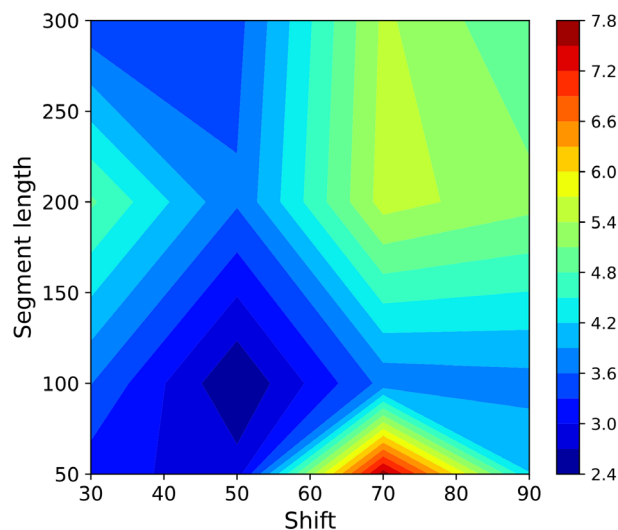


**FIGURE 4** Contour plot illustrating the relationship between shift and segment length. The dark blue region indicates the minimum mean absolute error (MAE), representing a global minimum. Similarly, the dark red region indicates the maximum MAE. [Color figure can be viewed at [wileyonlinelibrary.com](https://onlinelibrary.wiley.com/doi/10.1002/app.56170)]

## 3 | RESULTS AND DISCUSSION

This work utilized a Random Forest-based time series model to develop a forecasting framework for melt pressure at the die in PLA bead foam extrusion. The RF regressor is a powerful ML technique renowned for its ability to handle complex and nonlinear relationships within data. We applied the RF model to diverse datasets created by varying the shift and time window parameters.

Both metrics,  $R^2$  and MAE, provide valuable insights into model performance. We opted to prioritize MAE for further analysis due to its sensitivity to variations in the shift and time window parameters. By focusing on MAE, we could distinguish precise changes in model performance resulting from modifications in these parameters. This approach enabled us to identify the optimal combination of shift and segment length that led to the most accurate and reliable forecasts of melt pressure at the die in the PLA bead foam extrusion process.

We conducted forecasting experiments using various combinations of segment lengths and suitable shifts to determine the optimal configuration for minimizing MAE. This comprehensive analysis allowed for a thorough examination of the impact of segment length on forecasting accuracy, providing valuable insights into the effectiveness of different segmentation strategies. Upon analyzing each combination of the shift and segment length parameters, our analysis reached a significant conclusion aimed at minimizing the average MAE. Notably,

**TABLE 2** Mean Absolute Error (MAE) for prediction of melt pressure at the Die for PLA bead foam extrusion using the  $\Delta t = 100$  time units and shift parameter = 50 for 5 s, 1 min, and 5 min in future.

Time in future	Shuffled			Unshuffled		
	One-column	All-column	All-column stats	One-column	All-column	All-column stats
5 s	3.58	0.82	0.07	3.19	3.33	2.28
1 min	10.91	1.62	5.31	5.83	0.12	3.02
5 min	24.45	1.88	13.18	10.84	0.17	4.65

our investigation revealed that the most promising combination for further analysis is a segment length of 100 with a shift parameter of 50. This particular configuration consistently exhibited superior forecasting performance, characterized by reduced MAE values across various experimental conditions. The choice of a segment length of 100 and a shift parameter of 50 was informed by several factors. First, this configuration strikes a balance between capturing sufficient temporal information within each segment and ensuring an appropriate level of overlap between adjacent segments. Additionally, the 50-unit shift enables the creation of multiple overlapping segments, facilitating model training while retaining temporal coherence in the data. Overall, this optimized combination has the potential to enhance forecasting accuracy and reliability in melt pressure prediction for PLA bead foam extrusion.

This observation is evident in the contour plot in Figure 4, where the dark blue region signifies the global minimum for MAE. Within this region, we identify the average MAE to be 2.41, which represents the minimum value across all parameter combinations tested. Consequently, for further analysis and model refinement, we opted to retain the shift parameter at 50 and the segment length at 100. This strategic decision is driven by the desire to capitalize on the optimal forecasting performance achieved within this region, thereby enhancing the accuracy and reliability of our predictive models for melt pressure at the die in PLA bead foam extrusion.

In this study, we conducted forecasts of the melt pressure at the die for three different time horizons: 5 s, 1 min, and 5 min into the future. These forecasting results are summarized in Table 2.

Table 2 provides a comprehensive overview of the MAE for each forecasting horizon, utilizing different datasets tailored for the analysis of time series data. The “One-column” section of the table presents forecasts based only on historical melt pressure data. On the other hand, the “All-column” section incorporates the historical data of all processing parameters to forecast the melt pressure at the die. Furthermore, the “All-

column stats” section includes the statistical description of all processing parameters to enhance forecasting accuracy and provide deeper insights into the predictive modeling process.

Predictions were also made on the training set to assess the model's performance. By comparing the accuracy of the predictions on the training set with those on the test set, we can see the presence of some overfitting, as the test error is larger than the training error, for example, for the 5 s ahead forecasting the MAE (shuffled) is 1.22 for the test set and 0.66 for the training set. This difference in accuracy indicates that the trained RF model exhibits a moderate amount of overfitting, whose magnitude depends on the time in advance of the prediction (see Supporting information (Data S1) for more details).

### 3.1 | Five seconds ahead forecasting

Initially, our approach involves forecasting the pressure at the die using a 5-s forecasting window. Here, we observe that the MAE is highly sensitive to our data. While we achieve  $R^2$  of 0.96 with an MAE of 1.22 for shuffled data, indicating a good fit, it's noteworthy that the model benefits from the randomness introduced by shuffling. However, even in the unshuffled scenario, as depicted in Figure 5, the model shows acceptable performance, with an  $R^2$  of 0.50 and an MAE of 0.07. This indicates that the unshuffled scenario closely resembles real-world conditions, where the model lacks knowledge about the remaining 20% of the data. Despite this limitation, the model's predictive capabilities remain robust, highlighting its efficacy in forecasting melt pressure at the die.

### 3.2 | One minute ahead forecasting

Expanding our analysis to encompass 1-min forecasting intervals enhances our ability to capture longer-term trends and insights within the system. By

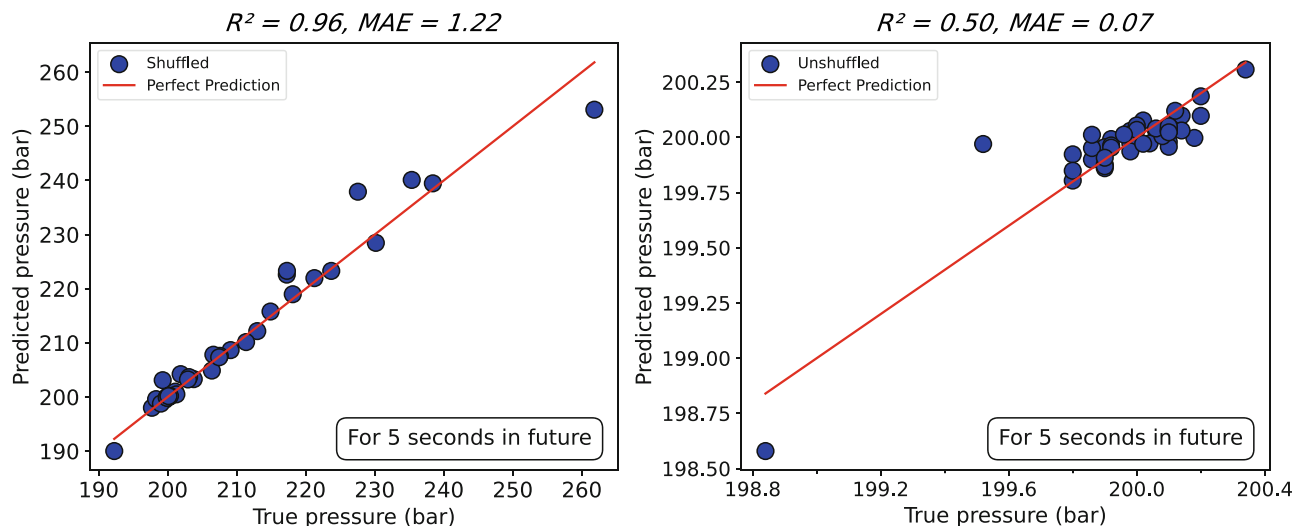


**FIGURE 5** Comparing true and predicted melt pressure values at the die, we analyze shuffled and unshuffled data. Specifically, we forecast melt pressure for a 5-s interval using 100 time steps (equivalent to 250 s) and a shift of 50. Evaluation metrics include (*MAE*) and ( $R^2$ ) after 5-fold cross-validation. [Color figure can be viewed at [wileyonlinelibrary.com](https://onlinelibrary.wiley.com/doi/10.1002/app.56170)]

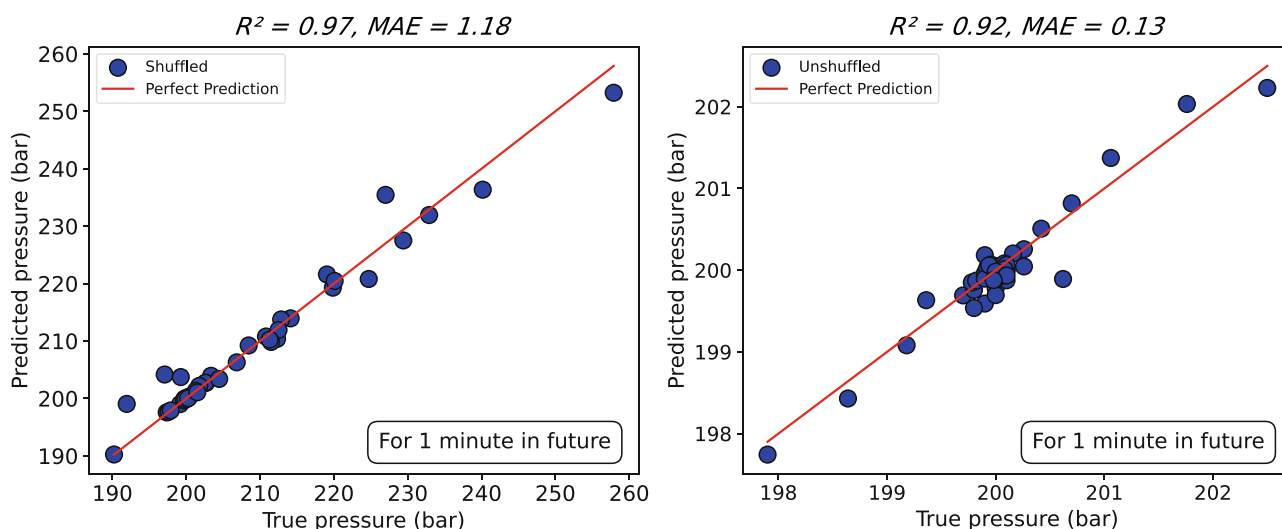


**FIGURE 6** Comparison between the true value and predicted value of the melt pressure at the Die for shuffle and unshuffle data. Forecasting the melt pressure at the die for 1 min ahead with the segment length of 100. The model is based on *MAE* and  $R^2$  score after 5-fold cross-validation. [Color figure can be viewed at [wileyonlinelibrary.com](https://onlinelibrary.wiley.com/doi/10.1002/app.56170)]

extending our predictions to cover a full minute, we gain a deeper understanding of the evolving dynamics. This broader scope enables more practical applications, as forecasting melt pressure 1 min into the future provides valuable insights into process trends. Our model demonstrates strong performance in this scenario, achieving an  $R^2$  score of 0.97 and an *MAE* of 1.18 for shuffled data, with similarly promising results for unshuffled data with an  $R^2$  score of 0.92 and *MAE* = 0.13. A parity plot can be seen in Figure 6 to compare the ML model performance.

### 3.3 | Five minutes ahead forecasting

Expanding our research horizon, we check the model with 5-min ahead forecasting, aiming to uncover a more significant understanding of the underlying processing dynamics. This extended time frame allows us to unveil precise patterns and trends that may avoid detection within shorter forecasting windows. Through rigorous analysis and experimentation, our objective is to decode the complex interplay of variables and their implications for future system states.



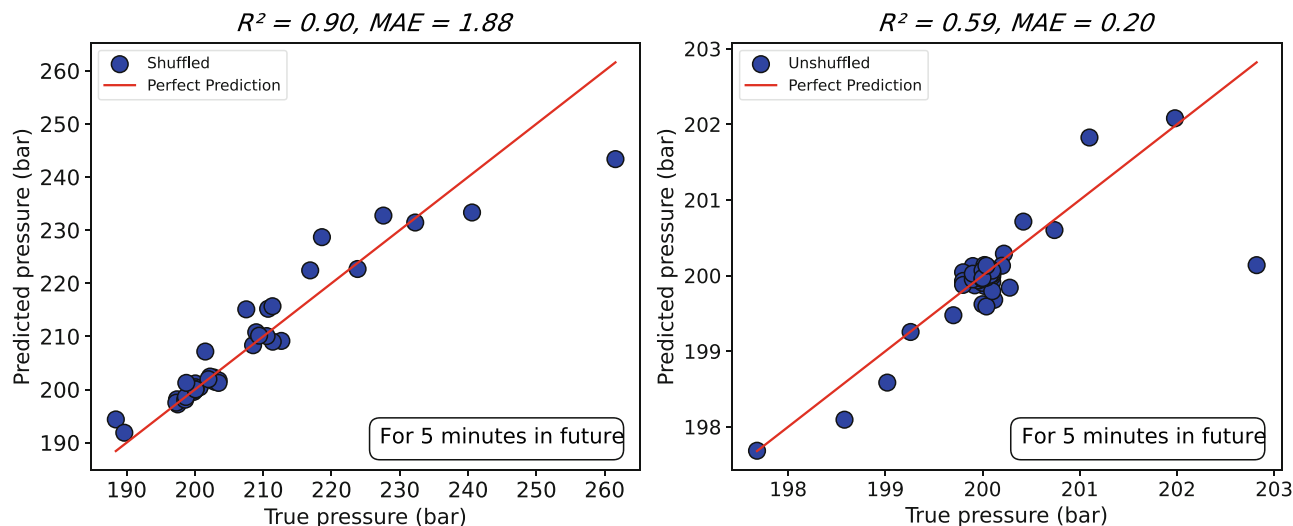


**FIGURE 7** Comparison between the true value and predicted value of the melt pressure at the Die for shuffle and unshuffle data. This include forecasting the melt pressure at the die for 5 min ahead with the segment length of 100. The model is based on  $MAE$  and  $R^2$  score after 5-fold cross-validation. [Color figure can be viewed at [wileyonlinelibrary.com](https://onlinelibrary.wiley.com/doi/10.1002/app.56170)]

Our exploration into 5-min forecasting offers valuable insights into the resilience and predictive capabilities of our models across varying temporal scales. Our model's proficiency in forecasting melt pressure over a 5-min horizon is evidenced by an  $R^2$  score of 0.90 and an  $MAE$  of 1.88 for shuffled data. Similarly, for unshuffled data, the model demonstrates strong forecasting performance, with an  $R^2$  score of 0.59 and an  $MAE$  of 0.20. These results can be seen in Figure 7 for more insight. These findings underscore the robustness and reliability of our forecasting approach, providing valuable guidance for real-world process optimization and decision-making.

## 4 | PRACTICAL IMPLEMENTATION IN INDUSTRY

Although the current work is a proof-of-concept investigation performed at an academic institution, we offer here a simplified discussion of points we consider important for implementing the AI model in industry. First, the RF model could be deployed in the same cloud service (e.g., Amazon Web Services, AWS) where the monitored extrusion signal is being stored. Every, say, 10 s, the signals of all parameters monitored for the last 100 time steps (or 500 s) would be combined and preprocessed (via a simple Python script running in the same AWS cloud) to exhibit the format/shape needed for predicting the die pressure. Whenever the predicted die pressure for example, 5 min in advance is outside the desired normal range of operation, either a message or a visual alert could be sent (also via the

Python script) to the operator in charge, so that he/she/they can make a decision on how to proceed, or a color signal could be sent to a local monitor. The operator could change the basic processing parameters of the operation or even shut down the equipment to decrease waste. If the extruder can be controlled from the cloud, another ML model (also deployed in the AWS cloud) could already suggest slight changes in some of the processing parameters, so that the predicted die pressure could be corrected to fall within the normal range, where no actions from the operator would be required.

## 5 | CONCLUSION

In this study, we successfully demonstrated the effectiveness of a time series-based machine learning approach for forecasting melt pressure at the die in PLA bead foam extrusion, a critical process parameter in this domain. Employing a random forest algorithm, we systematically explored various segmentation and shift parameters to identify the optimal configuration.

Our findings reveal that a segment length of 100 with a shift of 50 yields the highest forecast accuracy for melt pressure at the die. Additionally, we conducted a comprehensive statistical analysis, including key metrics such as mean, standard deviation, minimum, maximum, as well as the 25th, 50th (median), and 75th percentiles of the data, to evaluate its impact on model performance. Evaluation of the random forest model using both shuffled and unshuffled datasets demonstrated robust forecasting capabilities.

Furthermore, we assessed the model's performance across different time horizons: 5 s, 1 min, and 5 min ahead. For shuffled data, the model achieved an impressive  $R^2$  score of 0.96 with an  $MAE$  of 1.22, indicating a strong fit. Even in the unshuffled scenario, the model performed well, with an  $R^2$  score of 0.50 and an  $MAE$  of 0.07.

Similarly, strong performance was observed for 1-min and 5-min ahead forecasting, further highlighting the model's effectiveness across various forecasting horizons.

Overall, our study underscores the potential of time series-based machine learning techniques for forecasting critical process parameters in PLA bead foam extrusion. By using advanced algorithms and thorough data analysis, we provide valuable insights for process optimization and decision-making in this field, laying the groundwork for future advancements.

## AUTHOR CONTRIBUTIONS

**Karim Ali Shah:** Conceptualization (lead); data curation (lead); formal analysis (lead); investigation (lead); methodology (lead); visualization (lead); writing – original draft (lead). **Rodrigo Q. Albuquerque:** Supervision (equal); validation (lead); writing – original draft (supporting); writing – review and editing (lead). **Christian Brütting:** Investigation (equal); methodology (supporting); writing – review and editing (equal). **Holger Ruckdäschel:** Funding acquisition (lead); project administration (lead); writing – review and editing (lead).

## ACKNOWLEDGMENTS

The authors would be thankful to the German Research Foundation (DFG) for funding this project with grant number RU 2586/5-1. We extend our sincere gratitude for the financial support provided. Support from the “Bayerisches Staatsministerium für Wissenschaft und Kunst” under grant number F.2-M7426.10.2.1/4/16 in Germany is acknowledged. The support from Siemens AG is kindly acknowledged. Furthermore, special thank you to Andreas Himmelsbach, Marcel Dippold and Sebastian Gröschel for the deep insights about extrusion process. Open Access funding enabled and organized by Projekt DEAL.

## DATA AVAILABILITY STATEMENT

The data that support the findings of this study are available from the corresponding author upon reasonable request.

## ORCID

Holger Ruckdäschel  <https://orcid.org/0000-0001-5985-2628>

## ENDNOTE

<sup>1</sup> <https://plm.sw.siemens.com/en-US/insights-hub/>.

## REFERENCES

- [1] A. Ghosh, J. T. Orasugh, D. Chattopadhyay, S. S. Ray, *Specialty Polymers*, CRC Press, Boca Raton, Florida, United States **2023**, p. 295.
- [2] M. Tomin, Á. Kmetty, *J. Appl. Polym. Sci.* **2022**, *139*, 51714.
- [3] B. Mohammadi, A. Ershad-Langroudi, G. Moradi, A. Safaiyan, F. H. Kahnmauei, *Polymeric Foams: Applications of Polymeric Foams*, ACS Publications, Washington, DC **2023**, p. 253.
- [4] W. Gaojian, P. Xie, H. Yang, K. Dang, X. Yuxuan, M. Sain, L.-S. Turng, W. Yang, *J. Mater. Sci.* **2021**, *56*, 11579.
- [5] C. Brütting, T. Standau, J. Meuchelböck, P. Schreier, H. Ruckdäschel, *E-Polymers* **2023**, *23*, 20230092.
- [6] J. Kuhnigk, T. Standau, D. Dörr, C. Brütting, V. Altstädt, H. Ruckdäschel, *J. Cell. Plast.* **2022**, *58*, 707.
- [7] M. Jarpa-Parra, L. Chen, *Appl. Sci.* **2021**, *11*, 9605.
- [8] X. Lü, Y. Tingting, F. Meng, W. Bao, *Adv. Mater. Technol.* **2021**, *6*, 2100248.
- [9] S. S. Borkotoky, T. Ghosh, V. Katiyar, in *Advances in Sustainable Polymers. Materials Horizons: From Nature to Nanomaterials* (Eds: V. Katiyar, A. Kumar, N. Mulchandani), Springer, Singapore **2020**, [https://doi.org/10.1007/978-981-15-1251-3\\_12](https://doi.org/10.1007/978-981-15-1251-3_12)
- [10] X. Wang, J. Jang, S. Yanqun, J. Liu, H. Zhang, Z. He, Y. Ni, *J. Bioresour. Bioprod.* **2024**, *9*, 160.
- [11] L. Jiang, M. Sabzi, J. Zhang, *Applied Plastics Engineering Handbook: Processing, Sustainability, Materials, and Applications*, Elsevier, Amsterdam, Netherlands **2024**, pp. 133–165.
- [12] H. Nozari, J. Ghahremani-Nahr, A. Szmelter-Jarosz, *Advances In Computers*, Vol. 134, Elsevier, Philadelphia, Pennsylvania **2024**, p. 1.
- [13] T. Schuett, P. Endres, T. Standau, S. Zechel, R. Q. Albuquerque, C. Brütting, H. Ruckdäschel, U. S. Schubert, *Adv. Funct. Mater.* **2023**, *34*, 2309844.
- [14] G. Pilania, C. N. Iverson, T. Lookman, B. L. Marrone, *J. Chem. Inf. Model.* **2019**, *59*, 5013.
- [15] S. Oliver, L. Zhao, A. J. Gormley, R. Chapman, C. Boyer, *Macromolecules* **2018**, *52*, 3.
- [16] M. A. Morin, W. Zhang, D. Mallik, M. G. Organ, *Am. Ethnol.* **2021**, *133*, 20774.
- [17] A. J. Otaru, Z. A. Alhulaybi, I. Dubdub, *Polymer* **2024**, *16*, 437.
- [18] W. Yi, J. Guo, T. Zhou, H. Jiang, Y. Fang, *Appl. Acoust.* **2024**, *220*, 109966.
- [19] R. Q. Albuquerque, C. Brütting, T. Standau, H. Ruckdäschel, *E-Polymers* **2022**, *22*, 318.
- [20] S. Busra, C. Giuseppe, I. Gino, O. Mustafa, *Build. Acoust.* **2024**, Epub ahead of print, <https://doi.org/10.1177/1351010X24125495>
- [21] Y. Konuskan, A. H. Yilmaz, B. Tosun, I. Lazoglu, *Int. J. Adv. Manuf. Technol.* **2024**, *130*, 2957.
- [22] G. Akgun, O. Ulkir, *J. Thermoplast. Compos. Mater.* **2024**, *37*, 2225.
- [23] M. I. Pech-Mendoza, A. E. Rodríguez-Sánchez, H. Plascencia-Mora, *Proc. Inst. Mech. Eng. Part L: J. Mater. Des. Appl.* **2024**, *238*, 1331.
- [24] P. A. Withana, J. Li, S. S. Senadheera, C. Fan, Y. Wang, Y. S. Ok, *Environ. Pollut.* **2024**, *341*, 122833.

- [25] K. Zhang, Q. Wen, C. Zhang, R. Cai, M. Jin, Y. Liu, J. Y. Zhang, Y. Liang, G. Pang, D. Song, S. Pan, *IEEE Trans. Pattern Anal. Mach. Intell.* **2024**, 1.
- [26] X. Zheng, J. Yuan, Y. Liqiang, G. Wang, M. Zhu, *Int. J. Comput. Sci. Informat. Technol.* **2024**, 2, 18.
- [27] A. K. Dutta, M. Raparathi, M. Alsaadi, M. W. Bhatt, S. B. Dodda, M. Sandhu, J. C. Patni, *Multimed. Tools Appl.* **2024**, Epub ahead of print, <https://doi.org/10.1007/s11042-024-18918-1>
- [28] M. Mudassir, S. Bennbaia, D. Unal, M. Hammoudeh, *Neural Comput. & Applic.* **2020**, Epub ahead of print, <https://doi.org/10.1007/s00521-020-05129-6>
- [29] L. Lin, F. Wang, X. Xie, S. Zhong, *Expert Syst. Appl.* **2017**, 83, 164.
- [30] S. Pareeth, P. Karimi, M. Shafiei, C. De Fraiture, *Remote Sens.* **2019**, 11, 601.
- [31] Y. Mao, M. Hasan, C. Lee, M. N. T. Kilic, V. Gupta, W.-K. Liao, A. Choudhary, P. Acar, A. Agrawal, *2023 International Conference on Machine Learning and Applications (ICMLA)*, IEEE, Florida, USA **2023**, p. 890.
- [32] S. Luan, X. Xue, C. Wei, Y. Ding, B. Zhu, W. Wei, *Technol. Cancer Res. Treat.* **2023**, 22, 15330338231157936.
- [33] J. Andrews, O. Gkountouna, E. Blaisten-Barojas, arXiv preprint arXiv:2203.00151. **2022**.
- [34] K. A. Shah, C. Brütting, R. Q. Albuquerque, H. Ruckdäschel, *J. Appl. Polym. Sci.* **2024**, 141, e55693.
- [35] T. Standau, H. Long, *Materials* **2020**, 13, 1371.
- [36] S. L. Sclove, *Inf. Sci.* **1983**, 29, 7.
- [37] M. Lovrić, M. Milanović, M. Stamenković, *J. Contempor. Econom. Bus. Issues* **2014**, 1, 31.

## SUPPORTING INFORMATION

Additional supporting information can be found online in the Supporting Information section at the end of this article.

**How to cite this article:** K. A. Shah, R. Q. Albuquerque, C. Brütting, H. Ruckdäschel, *J. Appl. Polym. Sci.* **2024**, 141(44), e56170. <https://doi.org/10.1002/app.56170>